

RANDOM MUTAGENESIS OF HUMAN SERINE RACEMASE REVEALS RESIDUES IMPORTANT FOR THE ENZYMATIC ACTIVITY

Hillary E. HOFFMAN^{a1,b}, Jana JIRÁSKOVÁ^{a2,b}, Marketa ZVELEBIL^c and Jan KONVALINKA^{a3,b,*}

^a Gilead Sciences and IOCB Research Center, Institute of Organic Chemistry and Biochemistry, Academy of Sciences of the Czech Republic, v.v.i., Flemingovo nám. 2, 166 10 Prague 6, Czech Republic; e-mail: ¹ hehoffman@gmail.com, ² jana.jiraskova@uochb.cas.cz, ³ konval@uochb.cas.cz

^b Department of Biochemistry, Faculty of Science, Charles University in Prague, Hlavova 8, 128 43 Prague 2, Czech Republic

^c Breakthrough Breast Cancer Research Centre, The Institute of Cancer Research, 237 Fulham Road, London SW3 6JB, United Kingdom

Received January 13, 2010

Accepted January 13, 2010

Published online February 8, 2010

Human serine racemase (hSR) is a cytosolic pyridoxal-5'-phosphate dependent enzyme responsible for production of D-serine in the central nervous system. D-Serine acts as an endogenous coagonist of N-methyl-D-aspartate receptor ion channels. Increased levels of D-serine have been linked to amyotrophic lateral sclerosis and Alzheimer's disease, indicating that SR inhibitors might be useful tools for investigation or treatment of neurodegenerative diseases. However, despite hSR's promise as a therapeutic target, relatively few specific inhibitors have been identified, which is due in part to the lack of a three-dimensional structure of the enzyme. Here, we present a strategy for the generation and screening of random hSR mutants. From a library of randomly mutated hSR variants, twenty-seven soluble mutants were selected, expressed, and evaluated for enzymatic activity. Taking three carefully characterized mutants as an example, we show how this strategy can be used to pinpoint structurally and functionally important residues. In particular, we identify S84 and P111 as residues crucial for hSR activity and C217 and K221 as residues important for binding of the Mg²⁺ cofactor as well as for overall stability of the enzyme.

Keywords: D-Serine; Serine racemase; Error-prone PCR; Random mutagenesis; ThermoFluor assay; Enzymes; Racemases; Enzyme engineering; *In vitro* evolution.

Eukaryotic serine racemase (SR; EC 5.1.1.18) is a cytosolic pyridoxal-5'-phosphate (PLP) dependent enzyme responsible for the production of D-serine from L-serine and *vice versa*. In the mammalian central nervous system (CNS), D-serine acts as an endogenous coagonist of N-methyl-D-aspartate (NMDA) receptors, which are involved in glutamate-mediated excitatory neurotrans-

mission. In addition to its racemase activity, SR is also involved in serine metabolism by acting as a β -eliminase, converting L-serine¹⁻³, and to a lesser extent D-serine⁴, to pyruvate, with concomitant ammonia release. Both the racemization and elimination activities of mammalian SR are upregulated by divalent cations^{1,5}, ATP³, and reducing agents⁶.

Aberrant regulation of NMDA receptor mediated pathways has been implicated in a variety of neuropathologies, and excess D-serine production and overexpression of SR have been linked to Alzheimer's disease⁷ and amyotrophic lateral sclerosis⁸. While high-affinity NMDA receptor blockers are in clinical use, treatment of patients with these drugs is often accompanied by undesirable side effects such as hallucinations. In recent years, there has been a movement towards development of low-affinity NMDA receptor blockers that are both therapeutically effective and better tolerated by patients^{9,10}. In a similar manner, SR inhibitors might offer a more "gentle" approach to decrease NMDA receptor overactivation. Recently, Inoue and coworkers showed that amyloid- β -peptide mediated excitotoxicity is abrogated in SR knock-out mice¹¹, providing compelling evidence for the potential utility of SR inhibitors as therapeutic agents. However, very few competitive SR inhibitors have been described to date, and the most potent of these have K_i values in the micromolar range^{12,13}.

In order to design specific active-site-directed ligands with high potency and in order to gain a greater understanding of the catalytic and control mechanisms of this enzyme, it would be useful to determine the 3D structure of mammalian SR. While the structure of a SR orthologue from the fission yeast *Schizosaccharomyces pombe* (35.1%¹⁴ or 40%¹⁵ sequence identity to human SR) has been solved^{14,16}, the structure of a mammalian SR orthologue remains elusive. We therefore set out to establish a strategy for the generation and screening of human SR mutants in hopes of gaining insight into the structure-function relationships within the enzyme.

We have recently reported the heterologous expression of human SR (hSR) in *Escherichia coli* and purification and characterization of the recombinant enzyme¹⁷. In this work, we subjected the hSR gene to random mutagenesis by error-prone PCR and generated a plasmid library. The library was transformed into *E. coli*, and colonies expressing soluble hSR were detected with a dot-blot assay. For the initial analysis, twenty-seven soluble mutants were selected, expressed on a small-scale, partially purified, and evaluated for L-serine racemization and β -elimination activity. Three of these mutants – C217S, K221E, and S84G/P111L – were purified on a larger scale and analyzed in terms of thermal stability and activity. Multiple sequence alignment of 8 eukaryotic serine racemases and previously described homology

models^{17,18} were used to complement the experimental data and aid in assessing the potential function of the mutated residues.

EXPERIMENTAL

Abbreviations Used

CNS, central nervous system; DTT, 1,4-dithiothreitol; EP PCR, error-prone polymerase chain reaction; HEPES, 4-(2-hydroxyethyl)-1-piperazineethanesulfonic acid; IMAC, immobilized metal affinity chromatography; NiNTA, nickel nitrilotriacetic acid; NMDA, *N*-methyl-D-aspartate; PLP, pyridoxal-5'-phosphate; SR, serine racemase (hSR, human SR; mSR, mouse SR); TAE, tris-acetate ethylenediaminetetraacetic acid.

Error-Prone Polymerase Chain Reaction

The hSR gene was amplified under error-prone conditions from the plasmid pMPMhSR6His¹⁷. PCR reactions were set up according to two established protocols^{19,20}. In the first protocol, each reaction contained the template, 1 μ M forward primer, 1 μ M reverse primer, 4.2 mM MgCl₂, 0.5 mM MnCl₂ (molecular biology grade, Sigma), 1 μ l *Taq* DNA polymerase (New England Biolabs), and 1X Standard *Taq* (Mg-free) buffer. Four reactions were set up in parallel: in each, one dNTP was present at 3.4 mM, while the other three were added to final concentrations of 0.2 mM each. In the second protocol, the reactions contained the template, 1 μ M each primer, 5 mM MgCl₂, 1 μ l *Taq* DNA polymerase, 1X Standard *Taq* (Mg-free) buffer, 0.2 mM dITP (New England Biolabs), 20 μ M of one dNTP, and 0.2 mM of each of the three other dNTPs. The same thermal cycles were used for both protocols: an initial denaturation period of 5 min at 94 °C, followed by 16 cycles of 1 min at 94 °C, 1 min at 55 °C, and 3 min at 72 °C. The PCR products were run on a 1% TAE/agarose gel, and the appropriately-sized bands (approximately 1 kbp) were excised and purified with the QiaQuik Gel Extraction Kit (Qiagen) according to the manufacturer's instructions. The purified PCR products were combined and digested with *Nde*I and *Xho*I, then run on a 1% TAE/agarose gel, excised, and again purified with the QiaQuik kit. The mixture was ligated into pMPM-A4-2¹² digested with *Nde*I/*Xho*I using T4 DNA ligase, and 5 μ l of the ligation reactions were transformed into CaCl₂-competent *E. coli* MC1061.

Solubility Screening

The mutants were checked for soluble SR expression using a dot-blot protocol based on the work of Cornvik et al.²¹. Colonies were lifted using a nitrocellulose membrane, and the membrane was placed, colonies facing up, onto an LB/agar/ampicillin plate spread with 10 mM L-arabinose. SR expression was induced at 37 °C for 4 h. The nitrocellulose membrane with the colonies was then placed on top of a second nitrocellulose membrane and a piece of filter paper soaked in lysis buffer (50 mM phosphate buffer, pH 8.0, 300 mM NaCl, 20 μ M PLP, 1 mM MgCl₂, 5 mM 2-mercaptoethanol, 10 mM imidazole, 1 mg/ml lysozyme). The cells were subjected to 3 freeze-thaw cycles (10 min at -70 °C followed by 10 min at 37 °C). The upper nitrocellulose membrane was then discarded, while the lower membrane was incubated with Casein Blocker (Pierce, Rockford, Illinois) for 1 h, followed by overnight incubation with anti-SR antibody (1:500 dilution, BD Biosciences and/or antibodies produced in-house (un-

published results)). The membrane was then washed with PBS containing 0.05% TWEEN 20, incubated with horseradish peroxidase conjugated goat antimouse immunoglobulin (1:10,000, Pierce), then washed again. The blot was developed with SuperSignal WestPico chemiluminescence substrate (Pierce).

Mini-Purification and Characterization

Mutants expressing soluble SR variants were grown overnight in 10 ml cultures of auto-inducing ZYP-5052 broth²² supplemented with 0.05% arabinose and 100 μM ampicillin. The cultures were spun down, and the cell pellets were resuspended in lysis buffer and transferred to microcentrifuge tubes. After 30 min incubation at room temperature, the cells were sonicated 3×20 s. The insoluble fraction was pelleted by centrifugation at 16,000g, 4 °C, 20 min. The supernatant was then added to 100 μl NiNTA beads pre-equilibrated in wash1 buffer (same as lysis buffer but without lysozyme). After 30 min gentle rocking at room temperature, the NiNTA beads were allowed to settle to the bottom of the tube, and the “flow-through” fraction was removed. The beads were then washed once with 1 ml of wash1 buffer and twice with 1 ml of wash2 buffer (same as wash1 but with 30 mM imidazole). SR bound to beads was eluted with 500 μl elution buffer (containing 250 mM imidazole).

The eluted fractions were run on 12% SDS-PAGE and stained with Coomassie Brilliant Blue, and the purity of the preparations and quantity of SR present were accessed with ImageJ software (<http://rsb.info.nih.gov/ij>). Purified samples were then dialyzed against 100 mM HEPES, pH 8.0, containing 1 mM MgCl_2 and 10 μM PLP.

For activity reactions, ATP was added to the dialyzed samples to a final concentration of 1 mM, and DTT was added to 5 mM. Reactions were started by addition of 5 mM L-serine. After incubation at 37 °C for approximately 2 h, the reactions were quenched with perchloric acid and processed as described below. DNA for sequencing was prepared by growing single colonies overnight in 5 ml LB/ampicillin. Plasmids were purified from the cultured bacteria using the Spin Miniprep Kit from Qiagen. Sequencing was performed at the sequencing lab of the Faculty of Science of Charles University (Czech Republic) or at Macrogen (South Korea).

Large-Scale Purification

Plasmids were transformed into *E. coli* MC1061 and plated on LB/agar/ampicillin plates. Colonies were washed into Terrific Broth (12 g/l NZ amine, 24 g/l yeast extract, 0.4% glycerol, 0.017 M KH_2PO_4 , 0.072 M K_2HPO_4) containing 100 $\mu\text{g/l}$ ampicillin, and cultures were grown at 250–270 rpm and 37 °C until the OD_{600} reached 0.4–0.6. SR expression was then induced by addition of L-arabinose to a final concentration of 1 mM. After additional 4 h at 37 °C, cultures were harvested by centrifugation.

Lysis buffer was supplemented with Complete Mini EDTA-free Protease Inhibitor Tablets (Roche), and 5 ml were added per gram cells wet weight. After 20 min at ambient temperature, an additional 1 mg lysozyme per gram cells and DNaseI (0.1 mg per 100 ml lysate) were added, and the mixture was incubated at room temperature for another 20 min. The samples were then sonicated 3×20 s. The insoluble fraction was pelleted by centrifugation at 18,000g, 4 °C, 20 min. The purification was carried out on an ÄKTAprime FPLC (GE Healthcare). The soluble fraction was loaded onto NiNTA FastFlow resin (Qiagen) equilibrated with wash1 buffer. The column was washed with wash1 buffer until the A_{280} stabilized, then washed with wash2 buffer for a minimum of 10 column volumes or until the

A_{280} stabilized. Elution was carried out with a gradient of 30–250 mM imidazole over 30 ml; 2-ml fractions were collected. The fractions were analyzed by SDS-PAGE, and SR-rich fractions were pooled and extensively dialyzed against QA buffer (20 mM triethanolamine, pH 7.4, 20 μ M PLP, 1 mM $MgCl_2$, 0.1 mM DTT, 0.02% NaN_3).

Activity Assays

SR activity was analyzed in a pH 8.0 reaction buffer consisting of 100 mM HEPES–NaOH, 10 μ M PLP, 1 mM $MgCl_2$, and 1 mM ATP. Except where otherwise indicated, DTT was included at a concentration of 5 mM. For initial screening, a substrate concentration of 5 mM L-serine was used and reactions were started by addition of substrate. For determination of specific activity, 4 mM L-serine (Figs 5a and 5c) or 10 mM D-serine (Figs 5b and 5d) was used and reactions were started by addition of enzyme. Protein concentrations were determined by Bio-Rad Protein Assay (Bio-Rad Laboratories, California, USA). The enzymatic reactions were quenched with perchloric acid to precipitate SR, then neutralized with potassium hydroxide. For racemization analysis, the reaction mixture was derivatized by 1-fluoro-2,4-dinitrophenyl-5-L-alanine amide (Marfey's reagent, Pierce, USA) and resolved using reversed-phase HPLC as described¹. Pyruvate formation was determined by derivatization of reaction mixtures with 2,4-dinitrophenylhydrazine followed by resolution on reversed-phase HPLC as described¹².

Gel Filtration

Gel filtration was carried out on a Superdex200 HR 10/30 column (Pharmacia, Uppsala, Sweden) in QA buffer supplemented with 1 mM DTT and 150 mM NaCl. The following proteins were used as calibration standards: ferritin (440 kDa), aldolase (158 kDa), bovine serum albumin (67 kDa), ovalbumin (43 kDa), and chymotrypsinogen (25 kDa).

ThermoFluor Thermal Stability Assay

Reactions consisted of 35 μ l buffer solution, 10 μ l hSR (1.6–2 mg/ml), and 5 μ l 4X Sypro Orange dye (Sigma Aldrich). The total reaction volume was 50 μ l, and the final buffer composition was 100 mM HEPES (pH 8.0) and 10 μ M PLP. Where indicated, the buffer was supplemented with 1 mM ATP, 1 mM $MgCl_2$, 5 mM DTT, or a combination thereof. The reactions were heated from room temperature to 90 °C in a Light Cycler 480 Real-Time PCR machine (Roche). The excitation filter was set to 465 nm and the emission filter to 580 nm, and fluorescence measurements were recorded continuously. The data was analyzed with the accompanying software, and melting temperatures were calculated manually from the first derivatives.

Sequence Alignment

We performed multiple sequence alignment of SRs from 8 eukaryotic organisms (*Homo sapiens*, *Bos taurus*, *Rattus norvegicus*, *Mus musculus*, *Arabidopsis thaliana*, *Hordeum vulgare*, *Schizosaccharomyces pombe*, and *Saccharomyces cerevisiae*) using T-Coffee²³.

RESULTS AND DISCUSSION

Generation of a Library of Random Human Serine Racemase Mutants

Random mutagenesis is a valuable tool for protein modification, and a plethora of methods for producing mutated genes exists, including mutator *E. coli* strains, chemical reagents such as hydroxylamine, and error-prone polymerase chain reaction. A recent critical comparison of these methods suggests that EP PCR exhibits the widest operational range and highest degree of controllability²⁴. Furthermore, the authors suggest the use of a combination of EP PCR protocols in order to ensure a high level of diversity²⁴.

In this work, the plasmid pMPMhSR6His, which encodes hSR with a C-terminal 6-histidine tag¹⁷, was used as a template for EP PCR as described in detail in Experimental. We aimed for a mutation rate resulting in an average of 1–4 amino acid changes per mutant, and we employed two EP PCR protocols. The first, which involved varying the concentrations of the individual dNTPs and the addition of MnCl₂ to the reaction mixture¹⁹, resulted in a mutation rate of 2.3 mutations per 1000 base pairs (the hSR gene consists of 1040 base pairs), with 83% transition mutations (purine to purine or pyrimidine to pyrimidine) and 13% transversions (purine to pyrimidine or *vice versa*). Single nucleotide insertions or deletions were less frequent, comprising 4% of the total (all percentages based on sequencing data from 10,033 base pairs). The second protocol involved the use of various concentrations of dNTPs and the addition of dITP to the reaction mixture²⁰. This protocol resulted in a slightly higher mutation rate of 8.5 mutations per 1000 base pairs. Transition mutations were again favored, accounting for 80.7% of the total, while transversion mutations accounted for 19.3%. No insertions or deletions were observed in the 13,468 base pairs sequenced. The randomly mutated PCR products generated by both protocols were pooled, then digested with *Nde*I and *Xho*I and ligated into the arabinose-inducible vector pMPM-A4-2¹² to produce a plasmid library.

Library Screening

The plasmid library was transformed into *E. coli* MC1061. A colony dot-blot assay was employed to select colonies expressing soluble hSR variants, as illustrated in Fig. 1a. The assay was based on the colony filtration blot strategy reported by Cornvik et al.²¹, and procedures are described in detail in Experimental. Briefly, transformants were transferred onto a nitrocellulose membrane, and SR expression was induced with 10 mM L-arabinose. Fol-

lowing induction, the membrane with colonies bound was placed on top of a second nitrocellulose membrane and a piece of filter paper soaked in lysis buffer. The cells were lysed, which resulted in migration of the soluble proteins to the lower nitrocellulose membrane, while the insoluble fraction remained on the upper membrane. The lower membrane was then probed with anti-SR antibody in order to identify colonies producing soluble SR variants. This method appears to be quite robust, and we did not identify any false positives. However, in cases in which mutations occur within the antibody recognition site, the possibility of obtaining false negatives exists. We controlled for this possibility by probing the membranes with a mixture of anti-SR antibodies.

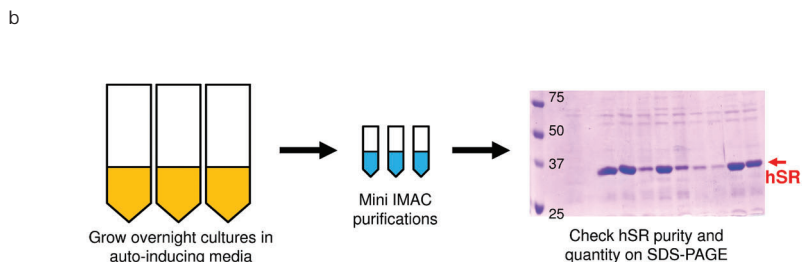
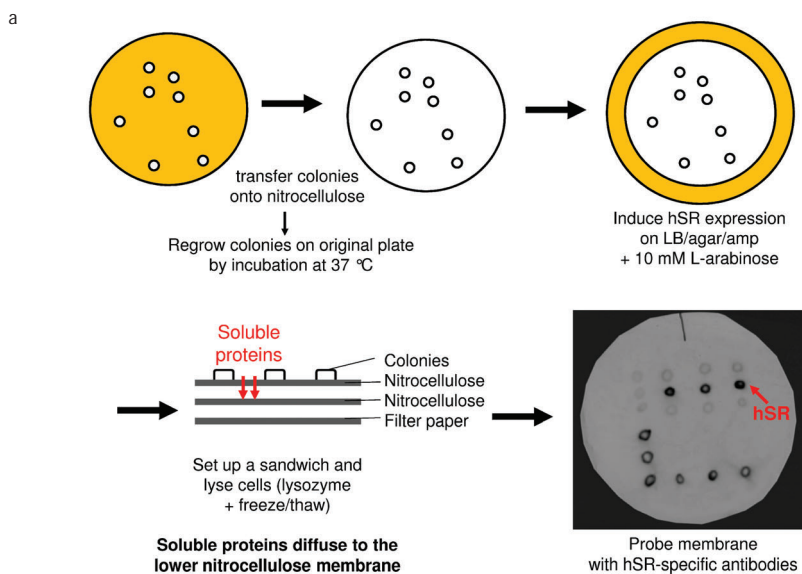


FIG. 1

Overview of the screening procedure. a Colony blot assay protocol, b Partial purification for activity measurements. Detailed procedures are given in Experimental

Twenty-seven positive colonies were picked from the original plates and grown overnight in 10 ml cultures of auto-inducing media. Small-scale purifications were carried out by immobilized metal affinity chromatography (IMAC) as shown in Fig. 1b. The IMAC-purified samples were then analyzed by SDS-PAGE to estimate hSR purity and quantity and subjected to activity analysis using our previously described HPLC-based endpoint assays^{1,12}. The activity reactions were carried out at pH 8.0 in the presence of the SR activators ATP, MgCl₂ and DTT, as described in Experimental. Both the L-serine racemization and elimination activities of the mutants were evaluated relative to wild-type hSR, and the results of the screening are shown in Table I and in Figs 2a and 2b. The mutants were divided into two

TABLE I
Summary of mutants identified by small-scale screening

Mutants with near-wild-type activity	Mutants with <50% wild-type activity
V12A	E133G/L176P
V138M	G39S/D132V
E129K/R277H/Q299H	V142A/I195V
S8Q	S84G/P111L*
K14M/N172D/M227L	K201R
L29M/K77R/V138E/I149T/E304V	S8G/E98G/K114T/K225R/F260L/K327R
T30S/M150L/I236V/I308V	D11G/F43S/V68A
N35D/Y231C/K306E/K327S	D112E/A120T/R253G
I23V/S32G	
V68G	
Mutants with 50–70% wild-type activity	Mutants with no measurable activity
S302P	K221E/T324A
L48P	V64I/G186S/G188S/E276K
I149T/Q272H	C217S
Q36L/R135H	K221E
E234G	

Mutants are divided into the following 4 categories based on L-serine racemization and elimination activity: near-wild-type activity, 50–70% wild-type activity, compromised activity (<50% of wild-type activity), and no measurable activity. Mutants selected for large-scale expression and purification are underlined. * No measurable racemization activity, but elimination activity was observed.

major categories – those that were active and those without measurable activity. The active mutants were further divided into three subcategories: mutants with near-wild-type activity, mutants that retained a substantial amount of activity (50–70% of the wild-type values), and mutants with compromised activity (<50% of the wild-type values) (see Table I).

1	2	3	4	5	6	7	8	9	10	11	12	13	14	15	16	17	18	19	20	21	22	23	24	25
M	C	A	Q	Y	C	I	S G	F	A	D G	V A	E	K M	A	H	I	N	I	R	D	S	I V	H	L
26	27	28	29	30	31	32	33	34	35	36	37	38	39	40	41	42	43	44	45	46	47	48	49	50
T	P	V	L M	T S	S	I	L	N	Q D	L Q	L	T	G S	R	N	L	F S	F	K	C	E	L P	F	Q
51	52	53	54	55	56	57	58	59	60	61	62	63	64	65	66	67	68	69	70	71	72	73	74	75
K	T	G	S	F	K	I	R	G	A	L	N	A	V I	R	S	L	V A G	P	D	A	L	E	R	K
76	77	78	79	80	81	82	83	84	85	86	87	88	89	90	91	92	93	94	95	96	97	98	99	100
P	K R	A	V	V	T	H	S	S G	G	N	H	G	Q	A	L	T	Y	A	A	K	L	E G	G	I
101	102	103	104	105	106	107	108	109	110	111	112	113	114	115	116	117	118	119	120	121	122	123	124	125
P	A	Y	I	V	V	P	Q	T	A	P L	D E	C	K T	K	L	A	I	Q	A T	Y	G	A	S	I
126	127	128	129	130	131	132	133	134	135	136	137	138	139	140	141	142	143	144	145	146	147	148	149	150
V	Y	C	E K	P	S	D V	E G	S	R H	E	N	V M E	A	K	R	V A	T	E	E	T	E	G	I M T	L
151	152	153	154	155	156	157	158	159	160	161	162	163	164	165	166	167	168	169	170	171	172	173	174	175
V	H	P	N	Q	E	P	A	V	I	A	G	Q	G	T	I	A	L	E	V	L	N D	Q	V	P
176	177	178	179	180	181	182	183	184	185	186	187	188	189	190	191	192	193	194	195	196	197	198	199	200
L	V	D	A	L	V	V	P	V	G	G S	G S	G S	M	L	A	G	I	A	I V	T	V	K	A	L
201	202	203	204	205	206	207	208	209	210	211	212	213	214	215	216	217	218	219	220	221	222	223	224	225
K	P	S	V	K	V	Y	A	A	E	P	S	N	A	D	D	C	Y	Q	S	K E	L	K	G	K R
226	227	228	229	230	231	232	233	234	235	236	237	238	239	240	241	242	243	244	245	246	247	248	249	250
L	M	P	N	L	Y C	P	P	E G	T V	I V	A	D	G	V	K	S	S	I	G	L	N	T	W	P
251	252	253	254	255	256	257	258	259	260	261	262	263	264	265	266	267	268	269	270	271	272	273	274	275
I	I	R G	D	L	V	D	D	I	F L	T	V	T	E	D	E	I	K	C	A	T	Q H	L	V	W
276	277	278	279	280	281	282	283	284	285	286	287	288	289	290	291	292	293	294	295	296	297	298	299	300
E K	R H	M	K	L	L	I	E	P	T	A	G	V	G	V	A	A	V	L	S	Q	H	F	Q H	T
301	302	303	304	305	306	307	308	309	310	311	312	313	314	315	316	317	318	319	320	321	322	323	324	325
V	S	P	E V	V	K E	N	I V	C	I	V	L	S	G	G	N	V	D	L	T	S	S	I	T A	W
326	327	328	329	330	331	332	333	334	335	336	337	338	339	340										
V	K R S	Q	A	E	R	P	A	S	Y	Q	S	V	S	V										

FIG. 2a

Location of mutated sites in the hSR sequence. Primary amino acid sequence of human SR depicting all the mutation sites. Mutations occurring in SR variants that retained some activity in the initial screening experiments are highlighted yellow, while mutations occurring in inactive variants are highlighted green. Lysine 56 is in blue and residues coordinating Mg^{2+} are in red letters.

To predict the positions of the mutations in the 3D structure, we analyzed a previously described homology model of hSR¹⁷. The majority of the mutations occurred at residues predicted to be at or near the surface of the enzyme, and a large percentage of the mutations occurred in putative loop regions (see Fig. 2b). This observation is likely due to the fact that our screening procedure selects for soluble, well-expressing hSR variants. Amino acid substitutions in the enzyme core may result in more drastic structural changes, leading to insolubility or poor expression levels. To test this hypothesis, we selected 11 colonies with low or undetectable levels of soluble hSR expression for DNA sequencing. Of the 11 mutants, 2 contained frameshift mutations and 5 contained nonsense mutations. Three of the remaining 4 mutants had mutations at putative PLP binding residues. The final mutant contained 7 amino acid changes (G39V/L67F/V151A/K225R/M227V/T285S/W325R), including several mutations of residues predicted to occur in the interior of the protein.

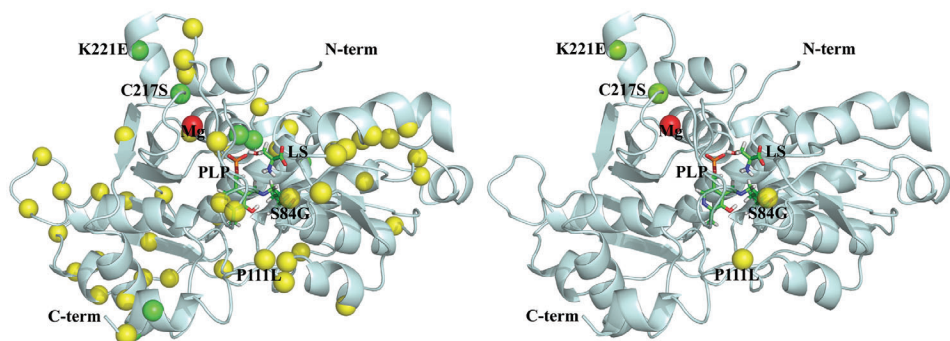


FIG. 2b

Location of mutated sites on the model. Homology model of hSR showing proposed locations of mutations. The picture on the left shows the positions of all observed mutations, and the picture on the right shows the positions of the studied mutations S84G, P111L, C217S, and K221E, which are labeled. Catalytically active mutations are shown as yellow spheres and inactive mutations as green spheres. PLP bound to Lys56 and the L-serine substrate are shown in sticks representation to enable visualization of the active site. The Mg^{2+} ion is shown as a red sphere. The figure was prepared with PyMol³⁵. The model depicted was built in Accelrys™ Discovery Studio 2.5 using the program MODELLER³⁶ with the *Schizosaccharomyces pombe* SR structure 2ZR8¹⁴ as a template. The modified PLP moiety [*N*-(5'-phosphopyridoxal)-D-alanine] present in the 2ZR8 structure was substituted in the homology model with unmodified PLP covalently bound to the N_ϵ atom of Lys56 by manual docking. The homology model of hSR was completed by adding the L-serine substrate and Mg^{2+} ion based on superposition with the 2ZR8 structure. Further computational refinement of the model was performed with AMBER 10 software³⁷ (unpublished data)

Based on our results from this limited screening, hSR seems to be remarkably tolerant of surface mutations. Several variants containing multiple mutations (up to 5 in the case of L29M/K77R/V138E/I49T/E304V) retained near-wild-type racemization and elimination activity. Even a SR variant bearing 6 mutations (S8G/E98G/K114T/K225R/F260L/K327R) was soluble and showed measurable serine racemization and elimination activity. It has been well-documented that mutations in surface patches can influence an enzyme ability to crystallize^{25,26}, and the random mutagenesis strategy outlined in this work could be extended in the future to identify hSR variants with an enhanced ability to form crystal contacts.

Few soluble mutants that effectively lacked both racemization and elimination activity were identified. The V64I/G186S/G188S/E276K mutant contains two mutations in the tetraglycine loop (Gly185–Gly188 in hSR), a common motif in PLP-dependent enzymes that stabilizes the phosphate moiety of the PLP cofactor. Destabilization of the PLP cofactor is a likely explanation for the activity loss. The K221E/T324A and K221E mutants were both inactive, pointing to the significance of lysine 221 for SR activity. The C217S hSR mutant was also inactive; C217S mouse SR has been previously reported to lack racemase activity, though the authors did not speculate about the reason for the activity loss²⁷. We found the substantial activity loss brought about by the K221E and C217S single mutations intriguing, particularly since both residues are in the vicinity of the Mg²⁺ coordinating residues (Fig. 3).

The S84G/P111L mutant was somewhat of an outlier in the screening assay, since its racemization activity was more dramatically affected than its elimination activity. Furthermore, the S84G mutation is predicted to occur not at the surface of the molecule but rather within the active site of SR (see Fig. 2b). We set out to study these three interesting mutants – C217S, K221E, and the double mutant S84G/P111L – in more detail.

Large Scale Expression and Purification of Wild-Type, C217S, K211E, and S84G/P111L hSR

In order to produce a sufficient amount of protein for more detailed functional studies, we scaled up the expression of wild-type, C217S, K221E, and S84G/P111L His-tagged hSR (1.5–3 l of culture). Highly purified proteins were obtained by FPLC-assisted IMAC purification as described in Experimental. A yield of 0.8 mg purified wild-type hSR was obtained per liter of culture. Yields of the C217S, K221E, and S84G/P111L mutants were 1.52, 0.8, and 1.34 mg/l, respectively. The successful upscaled purification of

HomSap	-----	MCAQYCI-SF	ADVEKAHINI	RDSIHILT PVL	TSSILNQITG	RNLFFKCELF	49	
BosTau	-----	MCQYCI-SF	ADVEKAHINI	RDFIHILTPVL	TSSILNQITG	RNLFFKCELF	49	
RatNor	-----	MCAQYCI-SF	ADVEKAHINI	QDSVHILTPVL	TSSILNQIAG	RNLFFKCELF	49	
MusMus	-----	MCAQYCI-SF	ADVEKAHINI	QDSIHILTPVL	TSSILNQIAG	RNLFFKCELF	49	
AraTha	-----	ME ANREKYAADI	LSIKEAHDRI	KPYIHRTPVL	TSESLNSISG	RSLFFKCECL	52	
HorVul	-----	MGRSDDDGHS	TEGGQYAADI	NSIREARARI	APYVHKTPII	SSTSIDAIAI	QKLFFFKCECF	60
SchPom	-----	MSDNLVLPY	DDVASASERI	KKFANKTPVL	TSSVTNKPEV	AEVFFKCNF	50	
SacCer	-----	MIVPTY	GDVLDASNRI	KEYVNKTPVL	TSRLNDRLG	AQYIFKGNF	46	
			: . * . *	: * * * *	: * : *	: * * * *		
HomSap	QKTGSFKIRG	ALNAVRLVLP	DALERKPKAV	VTSSGNHGQ	ALTYAAKLEG	IPAYIWPQT	109	
BosTau	QKTGSFKIRG	ALNAIRGLIS	AHPEEKPRAV	VAHSSGNHGQ	ALSPAARLEG	IPAYIVVPET	109	
RatNor	QKTGSFKIRG	ALNAIRGLIP	DTLEGGPKAV	VTSSGNHGQ	ALTYAAKLEG	IPAYIWPQT	109	
MusMus	QKTGSFKIRG	ALNAIRGLIP	DTPEEKPKAV	VTSSGNHGQ	ALTYAAKLEG	IPAYIWPQT	109	
AraTha	QKGGAFKFRG	ACNAVLSLD-	-AEQAA-KGV	VTSSGNHAA	ALSLAAKIQG	IPAYIWPKG	109	
HorVul	QKAGAFKIRG	ASNSIFALD-	-DSQAA-KGV	VTSSGNHAA	AVALAAKIRG	IPAYIWPKN	117	
SchPom	QKMGAFKFRG	ALNALSQLN-	-EAQRK-AGV	LTFSSGNHAQ	AIALSAKILG	IPAKIIMPLD	107	
SacCer	QRVGAFFKFRG	AMNAVSKLS-	-DEKRS-KGV	IAFSSGNHAQ	AIALSAKLIN	VPATIVMPED	103	
	* : * * * * *	* * * : *	* . *	:: * * * * *	* * : * * :	* * * * *		
HomSap	APDCKKLAIQ	AYGASIVYCE	PSDESRENA	KRVTEETEGI	MVHNPQEPV	IAGQGTIALE	169	
BosTau	APNKGKLAIQ	AYGASIVYSE	QSEESRENI	KRIAEETEGI	MVHNPQEPV	IAGQGTIALE	169	
RatNor	APNKGKLAIQ	AYGASIVYSE	PSDESRENA	QRIIQETEGI	LVHNPQEPV	IAGQGTIALE	169	
MusMus	APNKGKLAIQ	AYGASIVYCD	PSDESREKVT	QRIMQETEGI	LVHNPQEPV	IAGQGTIALE	169	
AraTha	APKCKVDNVI	RYGGKVIWSE	ATMSSREEIA	SKVLQETGSV	LIHPYNDGRI	ISGQGTIALE	169	
HorVul	APAKKVENVR	RYGGQVWISD	VTMSSRESTA	KKVQETGAI	LIHPFNDKYT	ISGQGTIALE	177	
SchPom	APAEKVAATK	GYGGQVIMYD	RYKDDREKMA	KEISEREGLT	IIPPYDHPHV	IAGQGTAAKE	167	
SacCer	ARALKIAATA	GYGAHIIRYN	RYTEDREIQI	RQLAAEHGFA	LIPPYDHPDV	IAGQGTAAKE	163	
	* * * * *	* * : * * :	* . * * * :	* . :	* * * * *	* * * * *		
HomSap	VLNQVPLVDA	LVVPVGGGGM	LAGIAITVKA	LKPSVKVYAA	EPNSNDICYO	SKLKGELTFN	229	
BosTau	VLNQVPLVDA	LVVPVGGGGM	LAGIAITVKA	LRPSVKVYAA	EPNLNDICYO	SKLKGELTFN	229	
RatNor	VLNQVPLVDA	LVVPVGGGGM	VAGIAITIKT	LKPSVKVYAA	EPNSNDICYO	SKLKGELTFN	229	
MusMus	VLNQVPLVDA	LVVPVGGGGM	VAGIAITIKA	LKPSVKVYAA	EPNSNDICYO	SKLKGELTFN	229	
AraTha	LLEQIQEIDA	IVVPISSGGL	ISGVALAASK	IKPSIRILAA	EPKGDIDSAQ	SKVAGKII-T	228	
HorVul	LLEQVPEIDT	IVVPISSGGL	ISGVTLAAKA	INPSIRILAA	EPKGDIDSAQ	SKAAGRII-K	236	
SchPom	LFEVVGPLDA	LFVCLGGGGL	LSGSALAAARH	FAPNCEYVGV	EPKANNDICQ	SFRKGSIV-H	226	
SacCer	LLEEVGQLDA	LFVPLGGGGL	LSGSALAAAS	LSPGCKIFGV	EPKANNDICQ	SFRSGSIV-H	222	
	: : * : * :	* * : * * * * :	* * * * :	* . : * * :	* * * * *	* * * * *		
HomSap	LYPPETIADG	VKS-SIGLNT	WPIIRDLVDD	IFVTVEDEIK	CATQLVWERM	KLLIEPTAGV	288	
BosTau	PYPPETIADG	IKS-SIGLNT	WPIIRDLVDD	VFTVTEDEIK	YATQLVWERM	KLLIEPTAGV	288	
RatNor	LHPPETIADG	VKS-SIGLNT	WPIIRDLVDD	VFTVTEDEIK	YATQLVWERM	KLLIEPTAGV	288	
MusMus	LHPPETIADG	VKS-SIGLNT	WPIIRDLVDD	VFTVTEDEIK	YATQLVWERM	KLLIEPTAGV	288	
AraTha	LPVTNTIADG	LRA-SIGDLT	WPVVRDLVDD	VTVLEECEII	EAAMKCYEIL	KVSPSPGAI	287	
HorVul	LPATSTIADG	LRA-FLGDLT	WPVVRDLVDD	VTVLEEDNAIV	EAAMKCYETL	KVAEPPSGAI	295	
SchPom	IDTPKTIADG	AQTQHLGNYT	FSIIEKEVDD	ILTVSDEELI	DCIKFYAARM	KIVVEPTGCL	286	
SacCer	INTPKTIADG	AQTQHLGEYT	FAIIRENVDD	ILTVSDQELV	KCMHFIAERM	KVVVEPTACL	282	
	: * * * * *	: : * * * * :	: : * * * * :	: : * * * * :	: : * * * * :	: : * * * * :		
HomSap	GVAAVLSQHF	QTVSPEV--K	NICIVLSGGN	VDLTSSITWV	KQ-AERPASY	QSVSV	340	
BosTau	GVAVVLSQHF	RTVPAEV--K	NICIVLSGGN	VDLTS-LTWV	KKQDEKAAE	-----	334	
RatNor	GLAAVLSQHF	QTVSPEV--K	NICIVLSGGN	VDLTS-LSWV	KQ-ERPAE	-----	333	
MusMus	ALAAVLSQHF	QTVSPEV--K	NVICIVLSGGN	VDLTS-LNWW	G-QAERPAPY	QTVSV	339	
AraTha	GLAAVLSNCF	RNNPSCRDCR	NIGIVLSGGN	VDLGS--LWD	SFKSSK----	-----	331	
HorVul	GLAAALSDEF	KQSSAWHESS	KIGIIVSGGN	VDLRV--LWD	SLYK-----	-----	337	
SchPom	SFAAARAMKE	----KLKKN	RIGIIVSGGN	VDMERYAHLF	SO-----	-----	323	
SacCer	GFAGALLKKE	----ELVVK	KVGIIVSGGN	VDKRYATLII	SGKEDGPTI-	-----	326	
	* . *		. : * : * * * *	* * :				

FIG. 3

Multiple sequence alignment of 8 eukaryotic serine racemases from *Homo sapiens* (HomSap), *Bos Taurus* (BosTau), *Rattus norvegicus* (RatNor), *Mus musculus* (MusMus), *Arabidopsis thaliana* (AraTha), *Hordeum vulgare* (HorVul), *Schizosaccharomyces Pombe* (SchPom), and *Saccharomyces cerevisiae* (SacCer). The sites of mutations S84G, P111L, C217S, and K221E are in yellow or in green (see legend to Fig. 2a); PLP binding Lys56 is in blue; residues coordinating Mg²⁺ are in red; hSR cysteines as well as conserved cysteines of other SR orthologues are in grey

these three mutants suggests that the results of our small-scale screening procedure are easily extendable to larger-scale applications.

All of the mutants contained an active-site-bound PLP based on spectrophotometric analysis. The oligomerization state of wild-type SR and the mutants was accessed by gel filtration on Superdex200HR as described in Experimental. The wild-type, K221E, and C217S mutants eluted as a single major peak corresponding to roughly 60 kDa, which is in accord with the results of Dunlop and Neidle³. While this is slightly lower than the predicted molecular weight of a SR dimer (74 kDa), it is significantly larger than the molecular weight of the monomer (37 kDa), and SR has been reported to form homodimers by several groups^{1,3,5}. Thus, we presume that wild-type, C217S, and K221E hSR are present in solution primarily in dimeric form. The S84G/P111L mutant also predominantly formed dimers, but significant amounts of higher molecular weight species (115 and 230 kDa) that might correspond to tetrameric and octameric species were also present.

Thermal Stability of C217S, K221E, and S84G/P111L hSR

The thermal stabilities of wild-type hSR and the C217S, K221E, and S84G/P111L mutants were assessed using ThermoFluor, a biophysical technique for determination of relative protein stabilities based on fluorophore partition into the denatured protein upon temperature increase²⁸⁻³⁰. In the absence of SR activators, wild-type, C217S, and K221E hSR exhibited melting temperatures of 63.2 ± 0.53 , 63.1 ± 0.17 , and 62.7 ± 0.32 °C, respectively. The S84G/P111L double mutant was slightly less stable, with $T_m = 61.6 \pm 0.40$ °C.

As illustrated in Fig. 4, addition of the known SR activators $MgCl_2$ and ATP (1 mM each) did not dramatically affect the melting temperature of wild-type or S84G/P111L hSR. On the other hand, the C217S and K221E mutants were stabilized by approximately 0.7 °C. Addition of $MgCl_2$ alone to these mutants had a similar effect, while addition of ATP alone did not cause significant stabilization (data not shown), suggesting that these mutants might be deficient in bound Mg^{2+} . Assessment of the thermal stability of the SR variants in the presence of 5 mM EDTA provided additional support for this hypothesis. Wild-type hSR and the S84G/P111L mutant were greatly destabilized by addition of EDTA with $\Delta T_m = -2.37$ and -3.54 °C, respectively. C217S and K221E hSR were only moderately affected with $\Delta T_m = -0.92$ and -0.41 °C, respectively (see Fig. 4).

The C217S and K221E mutants also showed altered sensitivity to reducing agents compared to wild-type and S84G/P111L hSR. Addition of 5 mM

DTT had a strong stabilizing effect on wild-type and the double mutant ($\Delta T_m = 3.4$ and 3.2 °C, respectively, compared to buffer alone). A comparable stabilizing effect could be achieved by addition of 2 mM tris(2-carboxylethyl)phosphine or 20 mM β -mercaptoethanol (data not shown). The requirement of free thiol groups for SR activity has been noted¹⁸, but the mechanism of SR stabilization and activation in reducing conditions is not yet understood. Human SR is a cysteine-rich protein containing 8 cysteine residues per monomer, yet there is no evidence indicating that disulfide bridges are present in the enzyme's native conformation. In fact, 5 of the cysteines are predicted to be surface-exposed. Sulfur in cysteine can adopt several redox states, and Cys is therefore involved in a number of functions and it is a common site for posttranslational modifications³¹. In the case of mouse SR, Mustafa et al.²⁷ have shown that modification at C113 can prevent ATP binding and activation. Addition of reducing agents to SR may prevent unwanted modifications and lead to protein stabilization by keeping the exposed cysteines in a reduced state. Another role for reducing agents could be prevention of irreversible oxidation of the enzyme. A recent review indicates that some PLP-containing enzymes can undergo paracatalytic side reactions with molecular oxygen or $\cdot\text{NO}$ radical, leading to

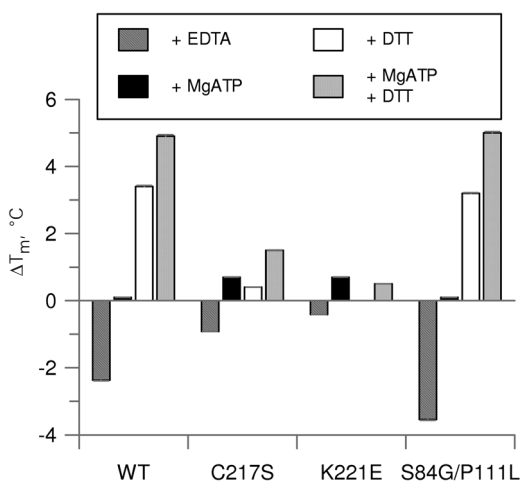


FIG. 4

Melting temperature changes (ΔT_m , °C) in the presence of various SR cofactors and additives. All samples contained 100 mM HEPES (pH 8.0) and 10 μM PLP. Samples labeled “+EDTA” contained 5 mM EDTA, “+MgATP” contained 1 mM MgCl_2 and 1 mM ATP, and “+DTT” were supplemented with 5 mM DTT

deactivation of the enzyme³². This mechanism of inactivation has been described for some decarboxylases, and it can be prevented by addition of thiols.

In contrast to the wild-type, the stabilities of the C217S and K221E mutants were not significantly affected by addition of DTT, which might suggest that these mutants are structurally different, perhaps due to their impaired Mg^{2+} binding abilities. Cook et al.⁵ have shown that the fluorescence spectra of EDTA-treated mSR and Ca^{2+} -saturated mouse SR are markedly different, suggesting that binding of the divalent cation causes a dramatic structural change. In almost all cases, the exception being the K221E mutant, the hSR variants exhibited the highest T_m values in the presence of all three activators, with wild-type being the most stable, followed by S84G/P111L, then C217S and K221E.

Kinetic Characterization of C217S, K221E, and S84G/P111L hSR

Since the thermal stability analyses indicated that the C217S and K221E mutants were differently affected by the presence of reducing agents than the S84G/P111L mutant and wild-type SR, we measured the specific activities of the purified SR variants in the presence and absence of 5 mM DTT. We have previously observed that wild-type SR purified and stored with a high concentration of DTT is not significantly affected by addition of DTT to the activity reaction, while SR purified and stored with low levels of DTT is activated by addition of DTT (unpublished results). To probe the effects of high concentrations of DTT on activity of the mutants, we stored the mutants and the wild-type in the presence of a low concentration of DTT (0.1 mM). All activity reactions were conducted in the presence of 1 mM $MgCl_2$, 1 mM ATP, and 10 μM PLP. Working with high concentrations of the purified proteins, we were able to detect a low level of serine racemization for all three mutants (Figs 5a and 5b). Wild-type SR was strongly activated in the presence of 5 mM DTT, with specific activity values 6- and 4-fold higher in the presence of DTT than in its absence for the L-serine to D-serine (Fig. 5a) and D-serine to L-serine (Fig. 5b) conversions, respectively. In contrast, none of the mutants were significantly activated by DTT.

The conversion of D-serine to pyruvate (Fig. 5d) is the least efficient of the four serine reactions catalyzed by SR, but it seems to be the most affected by DTT. The wild-type specific activity was 9-fold higher in the presence of DTT than in its absence, and all of the mutants were slightly activated (2- to 3-fold) by addition of DTT. As with the racemization reac-

tions, all of the mutants exhibited severely compromised activity compared to the wild-type.

A slightly different pattern was observed for the L-serine to pyruvate conversion (Fig. 5c). Again, all of the mutants are less active than wild-type hSR. The wild-type is activated 4-fold by addition of 5 mM DTT, while the C217S and K221E mutants exhibited compromised activity that could not be recovered by addition of DTT. However, in this case, the S84G/P111L mutant shows a 3-fold increase in specific activity upon addition of DTT. Recently, Goto et al.¹⁴ produced an S82A mutant of *S. pombe* SR (S82 corresponds to S84 of hSR), which reportedly lost racemization and D-serine dehydratase activity but retained a substantial amount of L-serine dehydratase activity (about 50% of the wild-type level). In contrast to their results, we observe that, even when activated by addition of DTT, the S84G/P111L hSR mutant still exhibits compromised L-serine dehydratase activity (about 10% of the wild-type value). Furthermore, we observe that S84G/P111L hSR

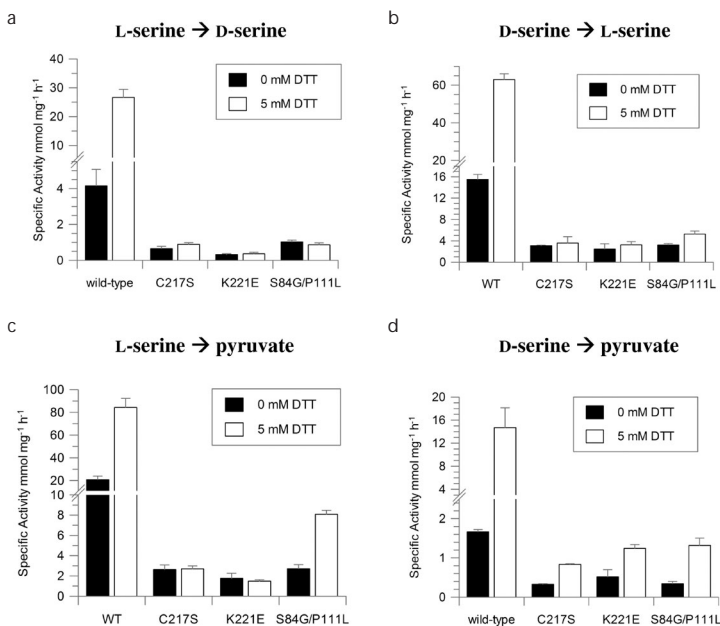


FIG. 5

Specific activity measurements. All reactions were conducted in the presence of 100 mM HEPES (pH 8.0), containing 1 mM PLP, 1 mM MgCl₂, and 1 mM ATP. Reaction mixtures were assayed by HPLC-based endpoint assay as described in Experimental. Specific activities are given in mmol of product evolved per mg of SR per hour. a) L-serine to D-serine, b) D-serine to L-serine, c) L-serine to pyruvate, and d) D-serine to pyruvate conversions

has detectable, albeit very modest, racemization and D-serine elimination activity. However, a direct comparison between S82A *S. pombe* SR and S84G/P111L hSR is not a fair one, since the Ser to Gly mutation is more extreme than the Ser to Ala mutation. Furthermore, we speculate that the additional mutation at P111 might cause further changes to the enzyme.

Multiple Alignment Analysis

We created a multiple sequence alignment of eight eukaryotic racemases (from *Homo sapiens*, *Bos taurus*, *Rattus norvegicus*, *Mus musculus*, *Arabidopsis thaliana*, *Hordeum vulgare*, *Saccharomyces cerevisiae*, and *Schizosaccharomyces pombe*) shown in Fig. 3. The alignment resembles that prepared by Baumgart et al.¹⁸, who compared human, plant, and yeast SRs with aspartate racemase from the bivalve mollusk *Scapharca broughtonii* and SR from the bacteria *Pyrobaculum islandicum*.

All eight homologues included in our alignment catalyze both serine racemization and elimination and are activated by Mg^{2+} ions. Most of these racemases are also activated by ATP, with the exception of SR orthologues from *Hordeum vulgare* (barley)³³ and *Arabidopsis thaliana*³⁴. Mammalian SRs exhibit a very high degree of sequence identity (84–91%), and we recently published a comparative study of the human and mouse orthologues¹⁷. Plant and yeast SRs boast a high level of sequence similarity to their mammalian orthologues (35–48% identity). Plant SRs have a 2–10 amino acid extension at the N-terminus, while both yeast and plant SRs are C-terminally truncated by 5–12 residues as compared to hSR. Predicted Mg^{2+} -binding residues are conserved throughout the family (residues depicted in red in Figs 2 and 3).

The only available experimentally determined structures of a eukaryotic serine racemase are four crystal structures of SR from fission yeast, *S. pombe* (PDB accession codes 2ZR8, 2ZPU, 1WTC, and 1V71)^{14,16}. Like hSR, *S. pombe* SR acts as both a racemase and an eliminase and is activated by divalent cations and ATP. Several homology models of mammalian SRs have been created based on these structures^{15,17}, and these models allow us to speculate about some features of the hSR structure and the potential structural effects of the mutations.

Cysteine 217 is conserved in mammalian SRs, while in yeast SRs the corresponding position is occupied by glycine. In SR from *Arabidopsis thaliana* the corresponding residue is an alanine, and in SR from *Hordeum vulgare* the position is occupied by a serine residue (see alignment in Fig. 3). In terms of sequence, Cys217 closely follows the magnesium coordinating residues

Glu210, Ala214, and Asp216. Conceivably, a mutation at residue 217 may disrupt the Mg^{2+} coordination site by altering intramolecular interactions in the vicinity.

Lys221 is also sequentially close to Mg^{2+} coordinating residues. Lys221 is conserved among mammalian SRs, while plant SRs bear arginine and yeast SRs glutamine in the corresponding position (see Fig. 3). The K221E mutation leads to reversal of the residue charge and might cause loss of a strong and possibly important salt-bridge interaction, leading to disruption of the coordination site topology.

Unlike the C217S and K221E mutants, the S84G/P111L mutant harbors mutations at two highly conserved residues. Ser84 is predicted to be located within the active site as part of a so-called “asparagine loop” (Ser83–His87), which has been shown to participate in substrate recognition and catalysis in *S. pombe* SR¹⁴. Thus, the S84G mutation in hSR likely directly affects the active site. The P111L mutation is predicted to occur within a short distance of the active site (Fig. 2b). P111 might be important for determining the correct orientation of the α -helix spanning residues Asp112–Tyr121 due to proline’s kink-forming propensity. It is possible that the proline to leucine mutation allows more flexibility in the orientation of the α -helix, which may in turn affect the active site topology and contribute to the impaired activity of the double mutant. In the absence of an experimentally determined mammalian SR structure, it is difficult to understand the observed change in the multimerization state of this mutant compared to the wild-type. The SR dimerization domain has been predicted based on the *S. pombe* SR structure¹⁵, but a potential tetramerization domain has not been identified. It is attractive to speculate that the residues close to the active site might control multimerization of the protein or that the multimerization state might affect the enzymatic activity. The behavior of the double mutant compared to the wild-type on the gel filtration column is the first evidence that the multimerization equilibria of SR can be shifted. More detailed structural studies will be needed to clarify the relationship, if any, between SR activity and multimeric state.

CONCLUSIONS

Random mutagenesis is a valuable toolbox for the biochemist. In this work, we describe a method for the generation and screening of random human serine racemase mutants. We identified and screened 27 hSR variants on a small scale, and we note, based on homology models, that the majority of the mutated sites are predicted to occur at or near the surface of the mole-

cule. This suggests that the method outlined here could be applied to the identification of active hSR mutants with altered surface properties, which in turn can be applied to the search for an hSR variant that forms well-diffracting crystals. In this work, we apply the method to the structure-activity analysis of SR by selecting 3 interesting mutants for large-scale expression and purification and a more detailed functional analysis. We conclude that neighboring residues C217 and K221, which are moderately conserved among eukaryotic SRs, are important for the racemization and elimination activities of hSR as well as the sensitivity of the enzyme to Mg^{2+} and reducing agents. The S84G/P111L mutant exhibits a thermal stability profile close to that of the wild-type, but both its racemization and elimination activities are severely impaired, suggesting that one or both of these residues might be directly involved in catalysis. Furthermore, the S84G/P111L mutant displays an altered multimerization state, suggesting the interesting possibility that multimerization plays a role in activity regulation.

Note added in the proof

In the time period between acceptance and publication of this manuscript, the human serine racemase X-ray structure was reported (Smith M. A., Mack V., Ebneth A., Moraes I., Felicetti B., Wood M., Schonfeld D., Mather O., Cesura A., Barker J.: *J. Biol. Chem.*, Epub ahead of print, doi:10.1074/jbc.M109.050062).

We would like to thank I. Nováková for her help with the screening and K. Grantz-Šašková, J. Brynda, and M. Lepšík for valuable discussions. We are grateful for the financial support provided by the Ministry of Education, Youth and Sports of the Czech Republic (Grant 1M0508).

REFERENCES

1. Strisovsky K., Jiraskova J., Barinka C., Majer P., Rojas C., Slusher B. S., Konvalinka J.: *FEBS Lett.* **2003**, 535, 44.
2. De Miranda J., Panizzutti R., Foltyn V. N., Wolosker H.: *Proc. Natl. Acad. Sci. U.S.A.* **2002**, 99, 14542.
3. Neidle A., Dunlop D. S.: *Neurochem. Res.* **2002**, 27, 1719.
4. Foltyn V. N., Bendikov I., De Miranda J., Panizzutti R., Dumin E., Shleper M., Li P., Toney M. D., Kartvelishvily E., Wolosker H.: *J. Biol. Chem.* **2005**, 280, 1754.
5. Cook S. P., Galve-Roperh I., Martinez del Pozo A., Rodriguez-Crespo I.: *J. Biol. Chem.* **2002**, 277, 27782.
6. Wolosker H., Sheth K. N., Takahashi M., Mothet J. P., Brady R. O., Jr., Ferris C. D., Snyder S. H.: *Proc. Natl. Acad. Sci. U.S.A.* **1999**, 96, 721.

7. Wu S. Z., Bodles A. M., Porter M. M., Griffin W. S., Basile A. S., Barger S. W.: *J. Neuroinflammation* **2004**, *1*, 2.
8. Sasabe J., Chiba T., Yamada M., Okamoto K., Nishimoto I., Matsuoka M., Aiso S.: *EMBO J.* **2007**, *26*, 4149.
9. Parsons C. G., Stoffler A., Danysz W.: *Neuropharmacology* **2007**, *53*, 699.
10. Lipton S. A.: *Nat. Rev. Drug Discov.* **2006**, *5*, 160.
11. Inoue R., Hashimoto K., Harai T., Mori H.: *J. Neurosci.* **2008**, *28*, 14486.
12. Strisovsky K., Jiraskova J., Mikulova A., Rulisek L., Konvalinka J.: *Biochemistry* **2005**, *44*, 13091.
13. Hoffman H. E., Jiraskova J., Cigler P., Sanda M., Schraml J., Konvalinka J.: *J. Med. Chem.* **2009**, *52*, 6032.
14. Goto M., Yamauchi T., Kamiya N., Miyahara I., Yoshimura T., Mihara H., Kurihara T., Hirotsu K., Esaki N.: *J. Biol. Chem.* **2009**, *284*, 25944.
15. Baumgart F., Mancheno J. M., Rodriguez-Crespo I.: *FEBS J.* **2007**, *274*, 4561.
16. Yamauchi T., Goto M., Wu H. Y., Uo T., Yoshimura T., Mihara H., Kurihara T., Miyahara I., Hirotsu K., Esaki N.: *J. Biochem.* **2009**, *145*, 421.
17. Hoffman H. E., Jiraskova J., Ingr M., Zvelebil M., Konvalinka J.: *Protein Expr. Purif.* **2009**, *63*, 62.
18. Baumgart F., Rodriguez-Crespo I.: *FEBS J.* **2008**, *275*, 3538.
19. Tarun A. S., Lee J. S., Theologis A.: *Proc. Natl. Acad. Sci. U.S.A.* **1998**, *95*, 9796.
20. Spee J. H., de Vos W. M., Kuipers O. P.: *Nucleic Acids Res.* **1993**, *21*, 777.
21. Cornvik T., Dahlroth S. L., Magnusdottir A., Flodin S., Engvall B., Lieu V., Ekberg M., Nordlund P.: *Proteins* **2006**, *65*, 266.
22. Studier F. W.: *Protein Expr. Purif.* **2005**, *41*, 207.
23. Notredame C., Higgins D. G., Heringa J.: *J. Mol. Biol.* **2000**, *302*, 205.
24. Rasila T. S., Pajunen M. I., Savilahti H.: *Anal. Biochem.* **2009**, *388*, 71.
25. Derewenda Z. S.: *Methods* **2004**, *34*, 354.
26. Price S. R., Nagai K.: *Curr. Opin. Biotechnol.* **1995**, *6*, 425.
27. Mustafa A. K., Kumar M., Selvakumar B., Ho G. P., Ehmsen J. T., Barrow R. K., Amzel L. M., Snyder S. H.: *Proc. Natl. Acad. Sci. U.S.A.* **2007**, *104*, 2950.
28. Nettleship J. E., Brown J., Groves M. R., Geerloff A.: *Methods Mol. Biol.* **2008**, *426*, 299.
29. Pantoliano M. W., Petrella E. C., Kwasnoski J. D., Lobanov V. S., Myslik J., Graf E., Carver T., Asel E., Springer B. A., Lane P., Salemme F. R.: *J. Biomol. Screen.* **2001**, *6*, 429.
30. Lo M. C., Aulabaugh A., Jin G., Cowling R., Bard J., Malamas M., Ellestad G.: *Anal. Biochem.* **2004**, *332*, 153.
31. Jacob C., Giles G. I., Giles N. M., Sies H.: *Angew. Chem. Int. Ed.* **2003**, *42*, 4742.
32. Bunik V. I., Schloss J. V., Pinto J. T., Gibson G. E., Cooper A. J.: *Neurochem. Res.* **2007**, *32*, 871.
33. Fujitani Y., Horiuchi T., Ito K., Sugimoto M.: *Phytochemistry* **2007**, *68*, 1530.
34. Fujitani Y., Nakajima N., Ishihara K., Oikawa T., Ito K., Sugimoto M.: *Phytochemistry* **2006**, *67*, 668.
35. DeLano W. L.: *The PyMol Molecular Graphics System*. DeLano Scientific, San Carlos (CA) 2002.
36. Eswar N., Marti-Renom M. A., Webb B., Madhusudhan M. S., Eramian D., Shen M., Pieper U., Sali A.: *Current Protocols in Bioinformatics*, Supplement 15. John Wiley & Sons, New York 2006.

37. Case D. A., Darden T. A., Cheatham III T. E., Simmerling C. L., Wang J., Duke R. E., Luo R., Crowley M., Walker R. C., Zhang W., Merz K. M., Wang B., Hayik S., Roitberg A., Seabra G., Kolossváry I., Wong K. F., Paesani F., Vanicek J., Wu X., Brozell S. R., Steinbrecher T., Gohlke H., Yang L., Tan C., Mongan J., Hornak V., Cui G., Mathews D. H., Seetin M. G., Sagui C., Babin V., Kollman P. A.: *AMBER 10*. University of California, San Francisco 2008.